PNAS
www.pnas.org

Supplementary Information for

The impact of rising CO_2 and acclimation on the response of US forests to global warming

John S. Sperry, Martin D. Venturas, Henry N. Todd, Anna T. Trugman, William R.L. Anderegg, Yujie Wang, and Xiaonan Tai

Corresponding author Martin D. Venturas
Email: martin.venturas@utah.edu

This PDF file includes:

Methods S1
Figs. S1 to S9
References for SI reference citations

Other supplementary materials for this manuscript include the following:

Datasets S1 to S7
Model Codes S1 to S2

www.pnas.org/cgi/doi/10.1073/pnas.1913072116

Brief description of Supplementary Information contents:

Methods S1. Algorithm for determining growing season length
Figure S1. Changes in growing season climatic conditions
Figure S2. Metabolic stress map for RCP4.5 and RCP8.5 scenarios
Figure S3. Leaf area index acclimation versus non-acclimated stress indicators
Figure S4. Trait acclimation versus growing season temperature increment
Figure S5. Changes in leaf area index, above ground biomass and maximum carboxylation capacity per ground area due to acclimation
Figure S6. Location of the selected sites
Figure S7. ESM selection based on mean annual temperature and precipitation changes for future (2070-2099) versus historic (1976-2005) periods
Figure S8. Changes in mean annual temperature and mean annual precipitation of the ESMs per region
Figure S9. Algorithm for determining the start and end of the growing season
Dataset S1. Characteristics of the selected sites and weather stations used in this study
Dataset S2. Earth System Models evaluated and selected for the simulations
Dataset S3. Species traits used for parameterizing the forest response model
Dataset S4. Climatic variables from the reference periods used for stand acclimation
Dataset S5. FLUXNET 2015 datasets used for testing the growing season length algorithm
Dataset S6. Hourly weather data used for running the simulations
Dataset S7. Main model output data from the 30 yr simulations
Code S1. Gain-risk model code in C++
Code S2. Acclimation routine code in Visual Basic

Supplementary Information Methods

Methods S1. Algorithm for determining growing season length.

The length of the growing season (GS) was determined from thermal time calculated as the cumulative degree-days above 5 °C from day of year 32 onwards (1). Cumulative degree days plotted vs. day of year follow a sigmoid shape (Fig. S9A) in the climates of the biogeographic regions analyzed in this study. The first day of the GS corresponded to the inflexion point where the cumulative thermal degree days began to increase rapidly (blue dashed line in Fig. S8A). The end of the GS end was set by the second inflexion point where the accumulation of thermal degree days rapidly slowed (red dashed line in Fig. S9A). The start and end dates were determined by fitting three lines with the lowest mean squared error to the sigmoidal plot of degree days vs. day of year (solid black lines in Fig. S9A). The GS start day was at the intersection of the first two lines (blue circle in Fig. S9A) and the GS end day was at the intersection of the last two lines (red square in Fig. S9A).

We tested the GS algorithm against gross primary productivity (GPP) from 11 sites of FLUXNEX 2015 dataset (http://fluxnet.fluxdata.org, Table S5). We used the daily data subsets (DD) of the FLUXNET 2015 sites. We used the mean daily temperature for the thermal degree-day calculations. We used the daily gross primary productivity from the nighttime partitioning method, with the reference calculated from model efficiency (GPP_NT_VUT_REF variable from FLUXNET 2015). For each of the years from the selected dataset we calculated the start and end of the GS and the percent of GPP of the year that occurred during the GS length. The mean percent of total annual GPP that was within the GS length determined by this algorithm was 77.1% for the 163 total years tested from all 11 sites. The percent GPP captured within the GS was highest for Morgan Monroe Sate Forest, Indiana, USA, with a mean of 91.8% for a 16 year period, and lowest for Metolious mature ponderosa pine stand, Oregon, USA, where only 51.0% of GPP was realized during the GS for a 13 record (Table S5). An example of how the GS start and end dates compare to GPP for years 200-2004 in Harvard Forest (42.5378 N, 72.1715 W, 340 m above sea level) is shown in Fig. S9B. For Harvard Forest 87.1 % of annual GPP for 1991-2012 period was captured by our GS algorithm.

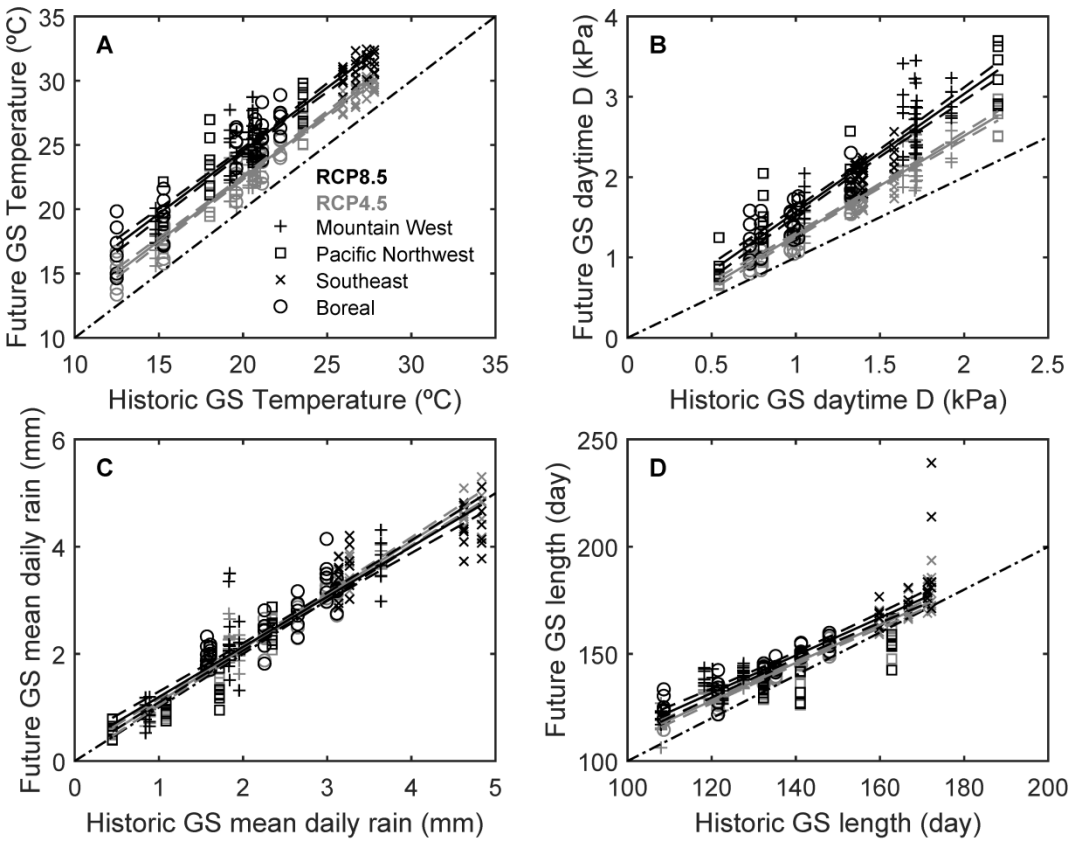

Fig. S1. Changes in growing season (GS) climatic conditions. Historic vs. future **(A)** mean GS temperature, **(B)** mean GS daytime atmospheric vapor pressure deficit (*D*), **(C)** mean GS daily precipitation, and **(D)** mean GS length. Regions: Mountain West, +; Pacific Northwest, square; Southeast, x; Boreal, circle. Scenarios: RCP4.5, grey (N=120); RCP8.5, black (N=120). Regressions (P<0.001), solid lines; 95% CIs, dash lines; 1:1, black dash-dot line.

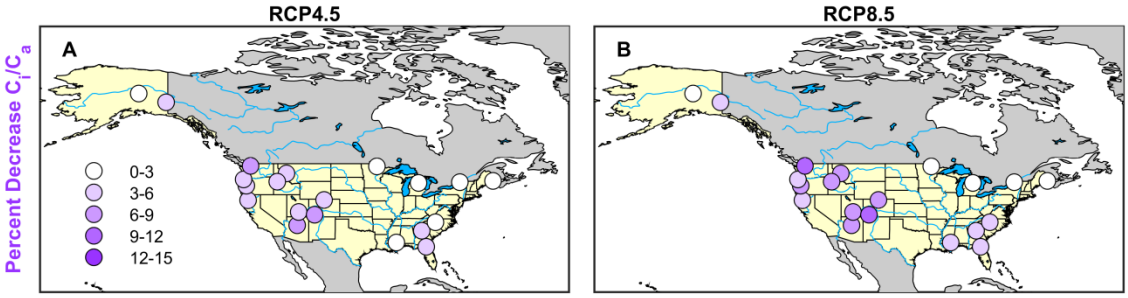

Fig. S2. Metabolic stress for non-acclimated stands represented as percent decrease in assimilation weighted internal to ambient CO_2 concentration ratio (C_i/C_a) for **(A)** RCP4.5 and **(B)** RCP8.5 scenarios. The drop in assimilation weighted C_i/C_a was larger for RCP8.5 scenario. Locations = 20; simulations per location = 6.

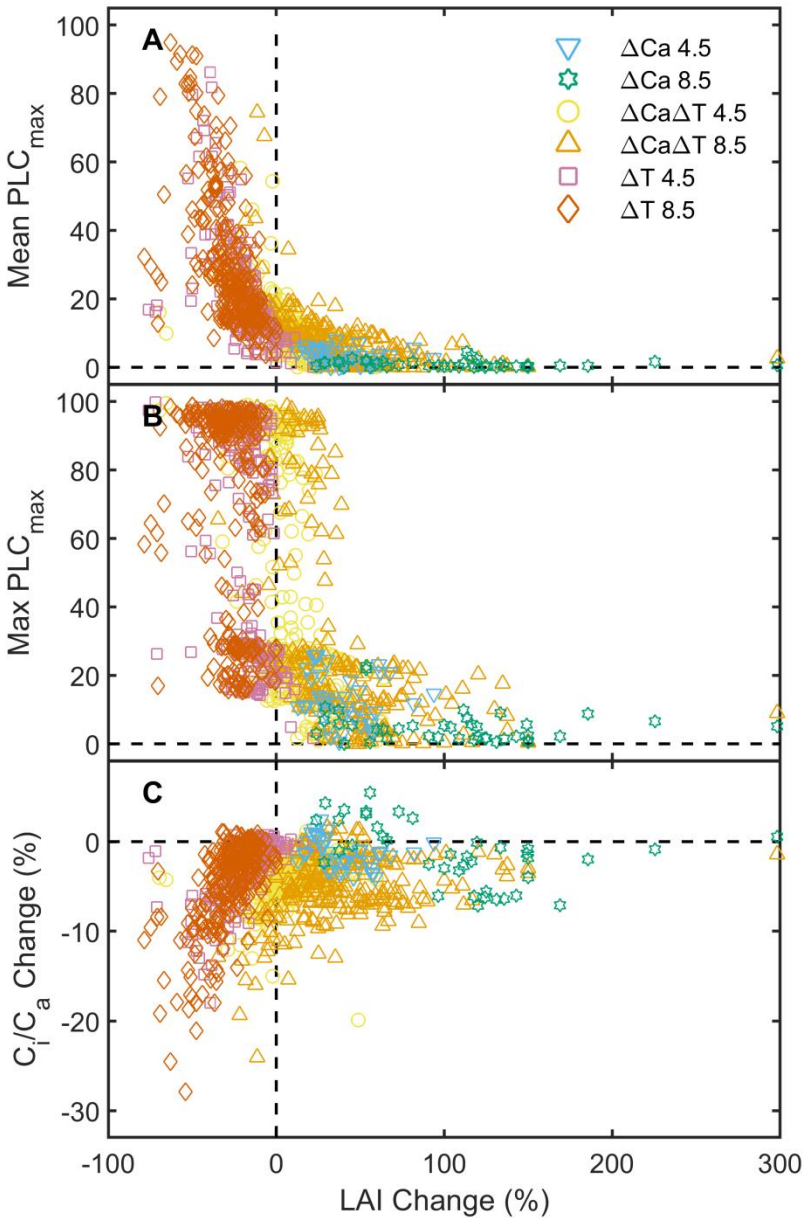

Fig. S3. Percent change in leaf are index (LAI) required for acclimation to ecohydrological equilibrium vs. the stress caused in the absence of such acclimation. **(A)** LAI change vs. mean PLC_{max}. **(B)** LAI change vs. maximum PLC_{max}. **(C)** LAI change vs. decrease in C_i/C_a (metabolic stress). Historic weather plus CO_2 enrichment to RCP4.5 (ΔC_a 4.5, blue downward circle, n=40) and RCP8.5 (ΔC_a 8.5, green star, n=40) levels, future scenarios with both warming and C_a enrichment ($\Delta C_a \Delta T$ 4.5, yellow circle, n=240; $\Delta C_a \Delta T$ 8.5, orange upward triangle, n=240), and warming only scenario (C_a at historic level) based on RCP4.5 (ΔT 4.5, pink square, n=240) and RCP8.5 weather simulations (ΔT 8.5, vermillion diamond, n=240).

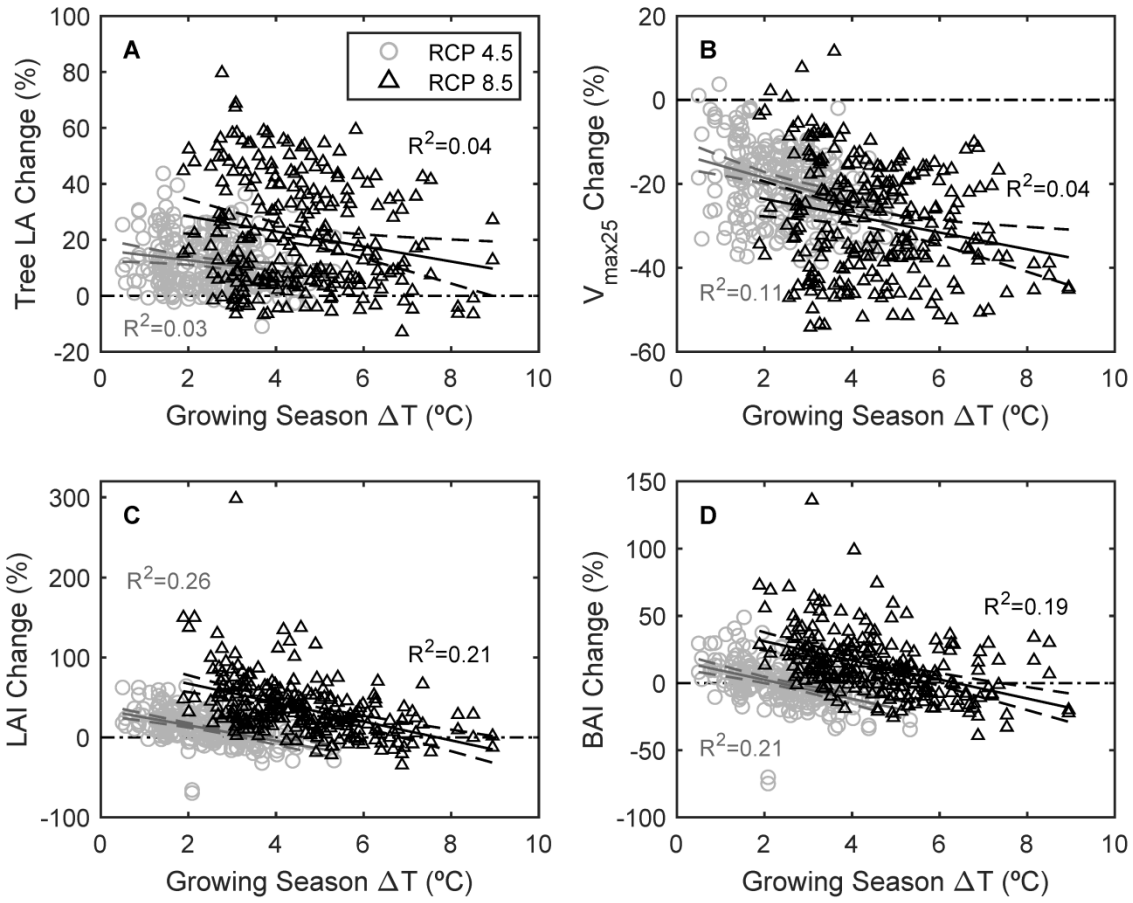

Fig. S4. Growing season temperature increment (ΔT) versus percent change in acclimated **(A)** tree leaf area (LA), **(B)** maximum carboxylation rate at 25 ºC (V_{max25}), **(C)** leaf area index (LAI), and **(D)** basal area index (BAI). Emission scenarios: RCP4.5 (grey circles) and RCP8.5 (black triangles). Black dash-dot lines, no change reference; solid grey lines, RCP4.5 regressions (95% CIs grey dashed lines); solid black lines, RCP8.5 regressions (95 % CIs black dashed lines). All regressions were significant ($P<0.01$; $n=240$).

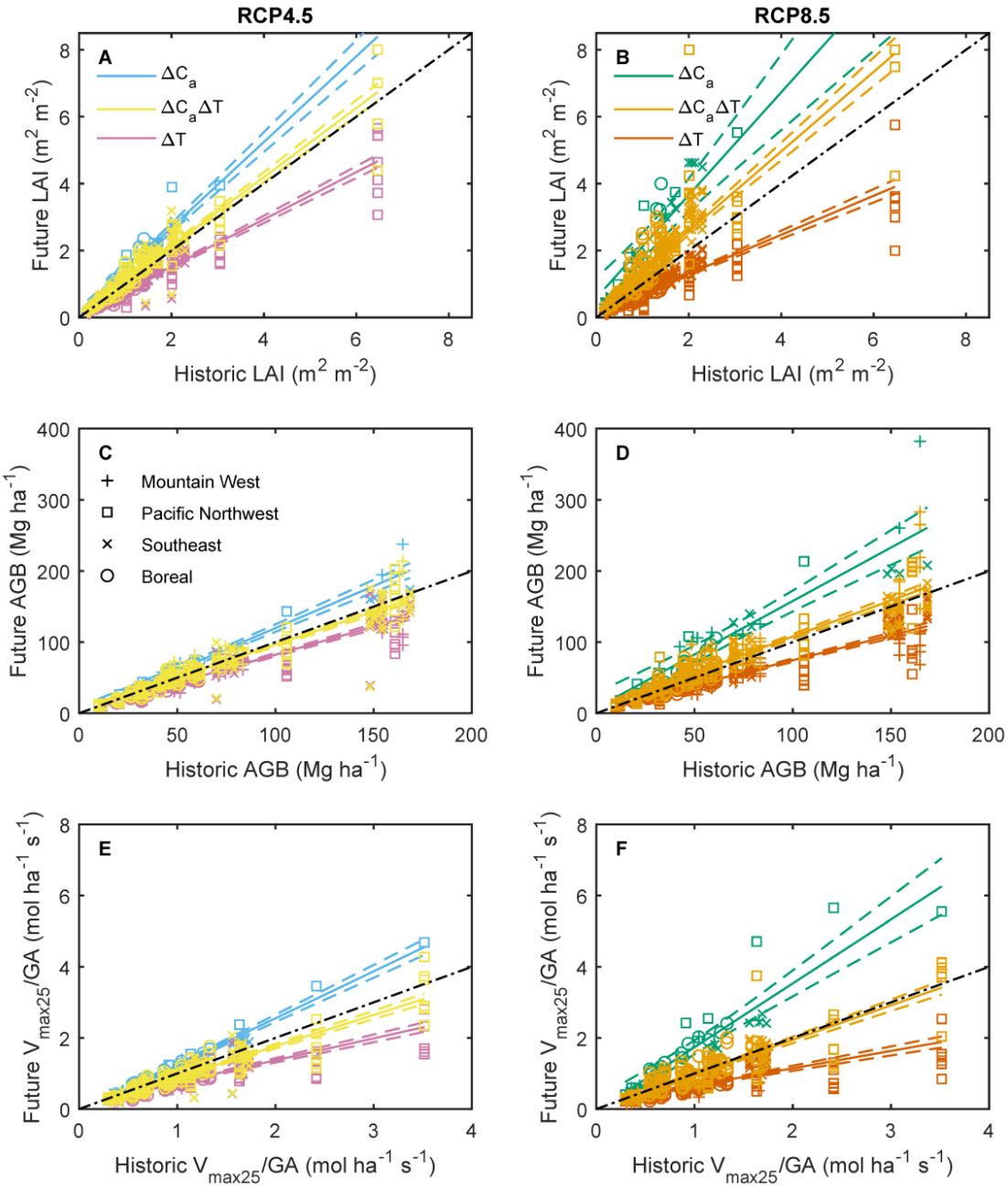

Fig. S5. Acclimated leaf area index (LAI), above ground biomass (AGB) and maximum carboxylation rate per ground area (V_{max25}/GA, an estimate of nitrogen requirements) for different weather and ambient CO_2 concentration (C_a) scenarios. **(A,B)** Historic vs. future LAI, **(C,D)** AGB, and **(E,F)** V_{max25}/GA for **(A,C,E)** RCP4.5 and **(B,D,F)** RCP8.5 projections. Treatments: C_a-enrichment only (ΔC_a, historic weather plus future C_a, blue for RCP4.5 and green for RCP8.5); C_a-enrichment plus warming ($\Delta C_a \Delta T$, future weather and future C_a, yellow for RCP4.5 and orange for RCP8.5); and warming only (future weather with historic C_a, ΔT, pink for RCP4.5 and vermillion for RCP8.5). Regions: Mountain West, +; Pacific Northwest, square; Southeast, x; and Boreal, circle. Solid lines: linear regressions; dashed lines: 95% confidence intervals; black dash-dot line: 1:1 relationship; ΔC_a (n=40), $\Delta C_a \Delta T$ (n=240) and ΔT (n=240).

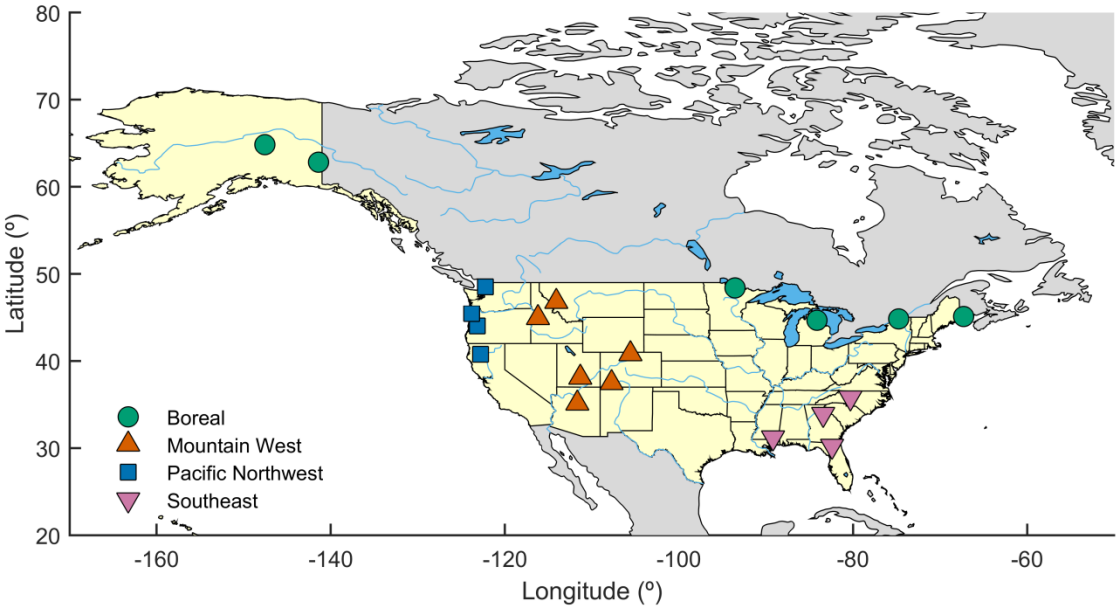

Fig. S6. Location of the 20 sites selected for this study from the four biogeographical regions: Boreal (green circle, n=4); Mountain West (vermillion upward triangle, n=6); Pacific Northwest (blue square, n=4); Southeast (pink downward triangle, n=4).

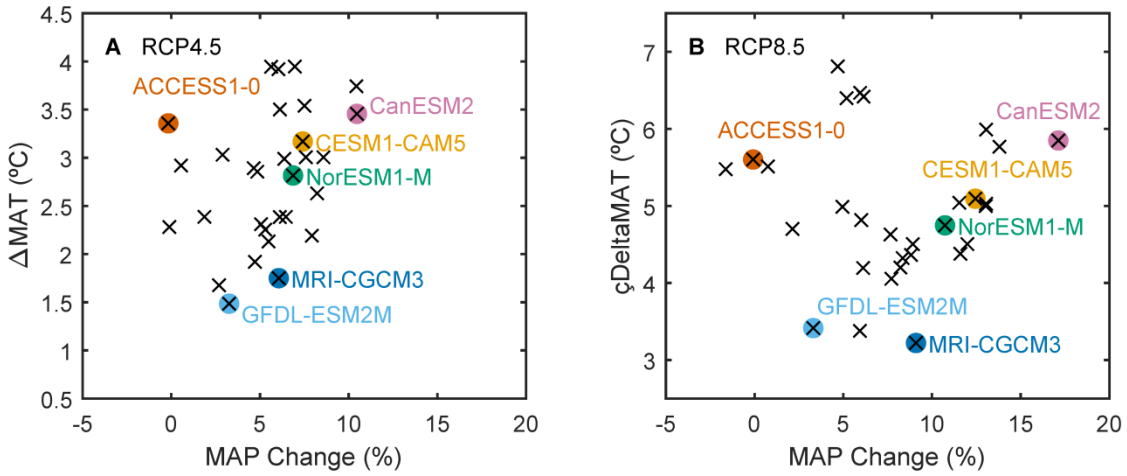

Fig. S7. Earth System Models (ESMs) selection based on mean annual precipitation (MAP) percent change and mean annual temperature (MAT) delta change for future (years 2070-2099) versus historic (years 1976-2005) periods. **(A)** Mean MAP and MAT across the 20 sites for the 30 ESMs evaluated for RCP4.5 and **(B)** RCP8.5 emission scenarios. The 30 ESMs (black crosses) and 6 models selected for this study (color circles) are represented in each panel. Based on their delta MAT and percent change in MAP models were characterized as *Warm-Dry* (ACCESS1-0), *Warm-Wet* (CanESM2), *Mean-1* (NorESM1-M), *Mean-2* (CESM1-CAM5), *Cool-Dry* (GFDL-ESM2M) and *Cool-Wet* (MRI-CGCM3).

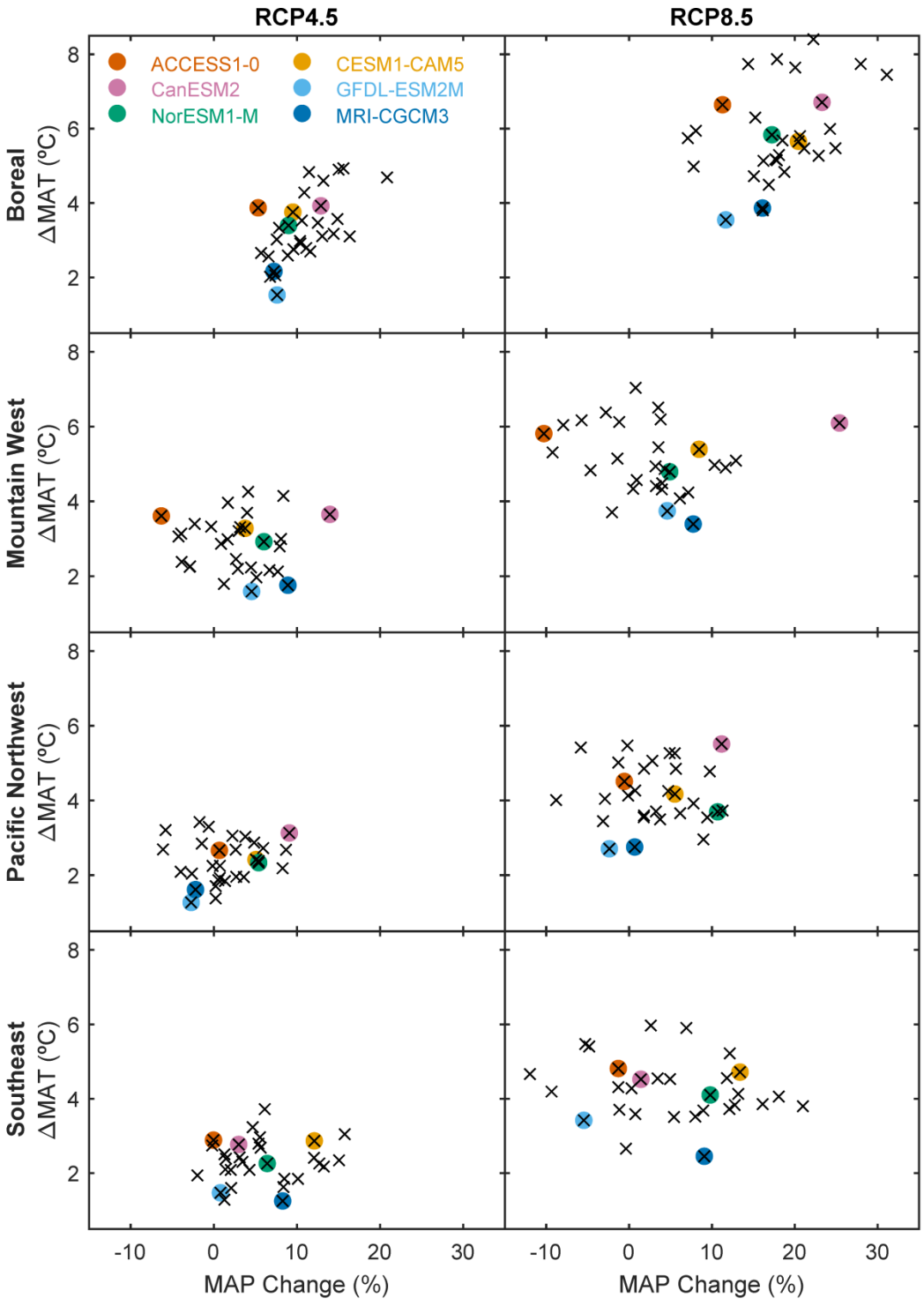

Fig. S8. Percent change in mean annual precipitation (MAP) and delta change in mean annual temperature (ΔMAT) for each biogeographical region and both emission scenarios. The 30 Earth System Models (black crosses) and 6 selected models for this study (color circles) are represented in each panel. Rows (top to bottom): Boreal, Mountain West, Pacific Northwest, and Southeast. Columns (left to right): RCP4.5 and RCP8.5 emission scenarios.

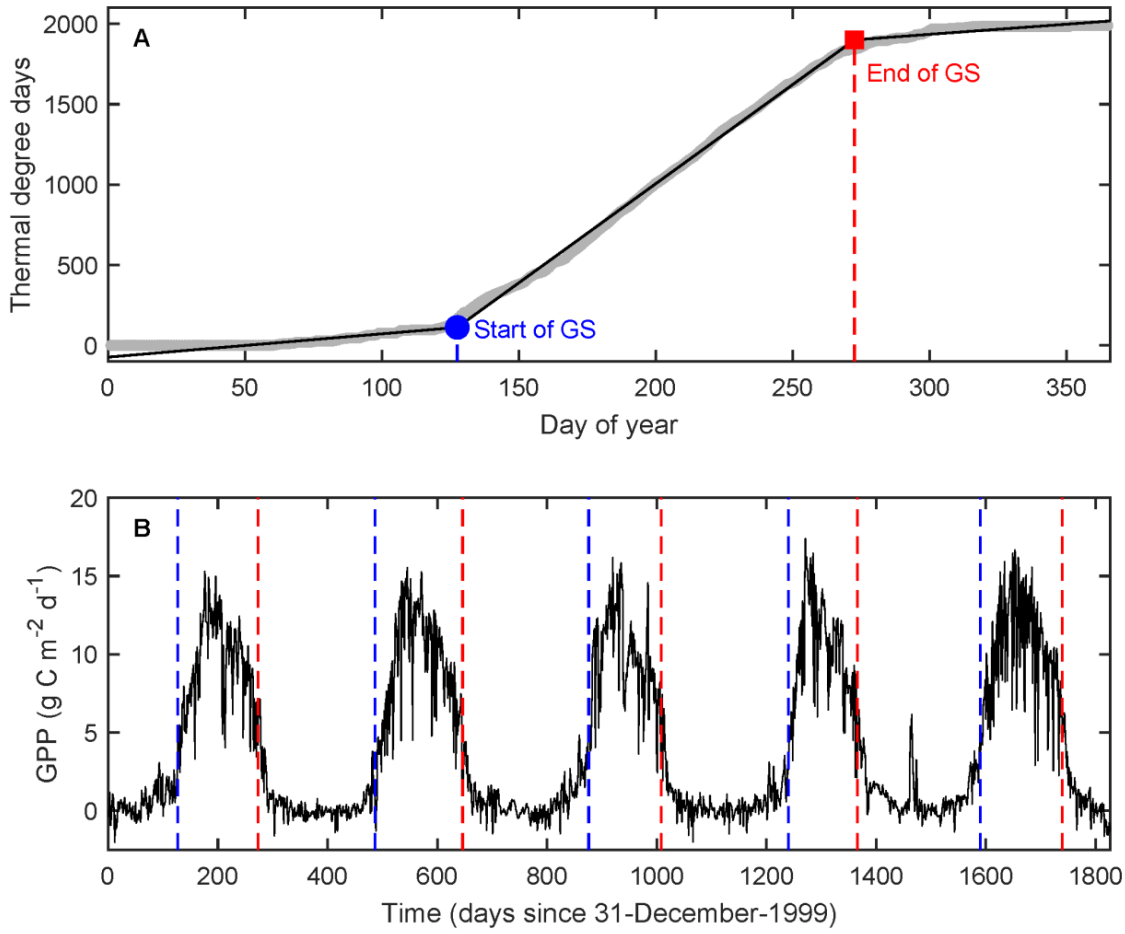

Fig. S9. Algorithm based on cumulative thermal degree days above 5 ºC for determining the start and end of the growing season (GS). **(A)** Cumulative degree days (grey line) for year 2000 GS at Harvard Forest and the GS start (dashed blue line) and end (red dashed line) days. The GS start and end days are determined by finding the intersections (blue circle and red square) between the three solid black lines that minimize the mean squared root error between the measured degree days and the line fit. **(B)** GS start (dashed blue lines) and end (dashed red lines) days calculated with the algorithm shown in panel A for growing seasons of years 2000-2004 versus gross primary productivity (GPP) from the FLUXNET 2015 Harvard Forest DATASET (https://doi.org/10.18140/flx/1440071). The algorithm captures the season when Harvard Forest is physiologically active.

Additional Datasets (separate files)

Dataset S1 (pnas201913072_s2_s1o1jh.xlsx). Characteristics of the selected sites and weather stations used in this study

Dataset S2 (pnas201913072_s3_s1o1jh.xlsx). Earth System Models evaluated and selected for the simulations

Dataset S3 (pnas201913072_s4_s1o1jh.xlsx). Species traits used for parameterizing the forest response model

Dataset S4 (pnas201913072_s5_s1o1jh.xlsx). Climatic variables from the reference periods used for stand acclimation

Dataset S5 (pnas201913072_s6_s1o1jh.xlsx). FLUXNET 2015 datasets used for testing the growing season length algorithm

Additional Datasets (separate files, Figshare DOI: 10.6084/m9.figshare.8805110)

Dataset S6. Hourly weather data used for running the simulations

Dataset S7. Main model output data from the 30 yr simulations

Additional Codes (separate files, Figshare DOI: 10.6084/m9.figshare.8805110)

Code S1. Gain-Risk model code in C++

Code S2. Acclimation routine code in Visual Basic

References (including references from SI Tables)

1. Fu YH, Campioli M, Deckmyn G, & Janssens IA (2012) The impact of winter and spring temperatures on temperate tree budburst dates: results from an experimental climate manipulation. *PLoS One* 7(10):e47324.
2. Burns RM & Honkala BH (1990) Silvics of North America: Volume 1. Conifers. Volume 2. Hardwoods. *United States Department of Agriculture (USDA), Forest Service, Agriculture Handbook 654*.
3. Pellis A, Laureysens I, & Ceulemans R (2004) Growth and production of a short rotation coppice culture of poplar I. Clonal differences in leaf characteristics in relation to biomass production. *Biomass Bioenergy* 27(1):9-19.
4. Martin JG, Kloeppel BD, Schaefer TL, Kimbler DL, & McNulty SG (1998) Aboveground biomass and nitrogen allocation of ten deciduous southern Appalachian tree species. *Can. J. For. Res.* 28(11):1648-1659.
5. Tripathi AM, *et al.* (2016) Evaluation of indirect measurement method of seasonal patterns of leaf area index in a high-density short rotation coppice culture of poplar. *Acta Universitatis Agriculturae et Silviculturae Mendelianae Brunensis* 64(2):549-556.
6. Lopez D, *et al.* (2013) Aquaporins and leaf hydraulics: poplar sheds new light. *Plant and Cell Physiology* 54(12):1963-1975.
7. Casella E & Ceulemans R (2002) Spatial distribution of leaf morphological and physiological characteristics in relation to local radiation regime within the canopies of 3-year-old Populus clones in coppice culture. *Tree Physiol.* 22(18):1277-1288.
8. Al Afas N, Pellis A, Niinemets Ü, & Ceulemans R (2005) Growth and production of a short rotation coppice culture of poplar. II. Clonal and year-to-year differences in leaf and petiole characteristics and stand leaf area index. *Biomass Bioenergy* 28(6):536-547.
9. Elias TS (1980) *The complete trees of North America. Field guide and natural history* (Van Nostrand Reinhold Company & Times Mirror Magazines Inc.).
10. Fan Y, Miguez-Macho G, Jobbágy EG, Jackson RB, & Otero-Casal C (2017) Hydrologic regulation of plant rooting depth. *Proceedings of the National Academy of Sciences*:201712381.
11. Jacobsen AL, *et al.* (2018) Intra-organismal variation in the structure of plant vascular transport tissues in poplar trees. *Trees* 32:1335-1346.
12. Jacobsen AL, Pratt RB, Venturas MD, & Hacke UG (2019) Large volume vessels are vulnerable to water-stress-induced embolism in stems of poplar. *IAWA Journal*.
13. Venturas MD, *et al.* (2019) Direct comparison of four methods to construct xylem vulnerability curves: differences among techniques are linked to vessel network characteristics. *Plant, Cell Environ.*:In Press.
14. Laur J & Hacke UG (2014) The role of water channel proteins in facilitating recovery of leaf hydraulic conductance from water stress in Populus trichocarpa. *PloS one* 9(11):e111751.
15. Olson ME, Aguirre-Hernández R, & Rosell JA (2009) Universal foliage-stem scaling across environments and species in dicot trees: plasticity, biomechanics and Corner's Rules. *Ecol. Lett.* 12(3):210-219.

16. Standish J, Manning GH, & Demaerschalk JP (1985) *Development of biomass equations for British Columbia tree species*.
17. Cairns MA, Brown S, Helmer EH, & Baumgardner GA (1997) Root biomass allocation in the world's upland forests. *Oecologia* 111(1):1-11.
18. Lavigne M & Ryan M (1997) Growth and maintenance respiration rates of aspen, black spruce and jack pine stems at northern and southern BOREAS sites. *Tree Physiol.* 17(8-9):543-551.
19. Marshall JD & Waring RH (1986) Comparison of methods of estimating leaf-area index in old-growth Douglas-fir. *Ecology* 67(4):975-979.
20. Peterson DL, Spanner MA, Running SW, & Teuber KB (1987) Relationship of thematic mapper simulator data to leaf area index of temperate coniferous forests. *Remote Sens. Environ.* 22(323-341).
21. Johnson DM, Woodruff DR, McCulloh KA, & Meinzer FC (2009) Leaf hydraulic conductance, measured in situ, declines and recovers daily: leaf hydraulics, water potential and stomatal conductance in four temperate and three tropical tree species. *Tree Physiol.* 29(7):879-887.
22. Bond BJ, Czarnomski NM, Cooper C, Day ME, & Greenwood MS (2007) Developmental decline in height growth in Douglas-fir. *Tree Physiol.* 27:441-453.
23. Manter DK & Kerrigan J (2004) A/Ci curve analysis across a range of woody plant species: influence of regression analysis parameters and mesophyll conductance. *J. Exp. Bot.* 55(408):2581-2588.
24. Committee (1993) *Flora of North America. Volume 2. Pteridophytes and Gymnosperms* (Oxford University Press).
25. Domec JC, Warren JM, Meinzer FC, Brooks JR, & Coulombe R (2004) Native root xylem embolism and stomatal closure in stands of Douglas-fir and ponderosa pine: mitigation by hydraulic redistribution. *Oecologia* 141(1):7-16.
26. Kavanagh KL, Bond BJ, Aitken SN, Gartner BL, & Knowe S (1999) Shoot and root vulnerability to xylem cavitation in four populations of Douglas-fir seedlings. *Tree Physiol.* 19:31-37.
27. Sperry JS & Ikeda T (1997) Xylem cavitation in roots and stems of Douglas-fir and white fir. *Tree Physiol.* 17(4):275-280.
28. Stout DL & Sala A (2003) Xylem vulnerability to cavitation in *Pseudotsuga menziesii* and *Pinus ponderosa* from contrasting habitats. *Tree Physiol.* 23:43-50.
29. Piñol J & Sala A (2000) Ecological implications of xylem cavitation for several Pinaceae in the pacific Northern USA. *Funct. Ecol.* 14:538-545.
30. Cade BS (1997) Comparison of tree basal area and canopy cover in habitat models: subalpine forests. *J. Wildl. Manage.* 61(2):326-335.
31. Bartelink H (1996) Allometric relationships on biomass and needle area of Douglas-fir. *For. Ecol. Manage.* 86(1-3):193-203.
32. Schultz RP (1997) Loblolly pine: the ecology and culture of loblolly pine (*Pinus taeda* L.). *Agriculture Handbook 713. Washington, DC: US Department of Agriculture, Forest Service. 493 p.*
33. Naidu SL, DeLucia EH, & Thomas RB (1998) Contrasting patterns of biomass allocation in dominant and suppressed loblolly pine. *Can. J. For. Res.* 28(8):1116-1124.

34. Cregg BM, Hennessey TC, & Dougherty PM (1990) Water relations of loblolly pine trees in southeastern Oklahoma following precommercial thinning. *Can. J. For. Res.* 20:1508-1513.
35. Domec J-C, *et al.* (2009) Decoupling the influence of leaf and root hydraulic conductances on stomatal conductance and its sensitivity to vapor pressure deficit as soil dries in a drained loblolly pine plantation. *Plant, Cell Environ.* 32:980-991.
36. Johnson DM, *et al.* (2016) A test of the hydraulic vulnerability segmentation hypothesis in angiosperm and conifer tree species. *Tree Physiol.* 36:983-993.
37. Myers DA, Thomas RB, & DeLucia EH (1999) Photosynthetic responses of loblolly pine (Pinus taeda) needles to experimental reduction in sink demand. *Tree Physiol.* 19:235-242.
38. Rogers A & Ellsoworth DS (2002) Photosynthetic acclimation of *Pinus taeda* (loblolly pine) to long-term growth in elevated pCO2 (FACE). *Plant, Cell Environ.* 25:851-858.
39. Shi K & Cao QV (1997) Predicted leaf area growth and foliage efficiency of loblolly pine plantations. *For. Ecol. Manage.* 95:109-115.
40. Ewers BE, Oren R, & Sperry JS (2000) Influence of nutrient *versus* water supply on hydraulic architecture and water balance in *Pinus taeda*. *Plant, Cell Environ.* 23:1055-1066.
41. Hacke UG, *et al.* (2000) Influence of soil porosity on water use in *Pinus taeda*. *Oecologia* 124:495-505.
42. Gill SJ, Biging GS, & Murphy EC (2000) Modeling conifer tree crown radius and estimating canopy cover. *For. Ecol. Manage.* 126:405-416.
43. Jokela EJ, Shannon CA, & White EH (1981) Biomass and nutrient equations for mature *Betula papyrifera* Marsh. *Can. J. For. Res.* 11(2):298-304.
44. Dillen SY, Beeck MO, Hufkens K, Buonanduci M, & Phillips NG (2012) Seasonal patterns of foliar reflectance in relation to photosynthetic capacity and color index in two co-occurring tree species, *Quercus rubra* and *Betula papyrifera*. *Agric. For. Meteorol.* 160:60-68.
45. Gower ST, Kucharik CJ, & Norman JM (1999) Direct and indirect estimation of leaf area index, f_{APAR}, and net primatry production of terrestrial ecosystems. *Remote Sens. Environ.* 70:29-51.
46. Sack L, Melcher PJ, Zwieniecki MA, & Holbrook NM (2002) The hydraulic conductance of the angiosperm leaf lamina: a comparison of three measurement methods. *J. Exp. Bot.* 53:2177-2184.
47. Wang Y, *et al.* (2019) The stomatal response to rising CO_2 concentration and drought is predicted by a hydraulic trait-based optimization model. *Tree Physiol.*
48. Sperry JS, Nichols KL, Sullivan JEM, & Eastlack SE (1994) Xylem embolism in ring-porous, diffuse-porous, and coniferous trees of northern Utah and interior Alaska. *Ecology* 75(6):1736-1752.
49. Kolb TE & Stone J (2000) Differences in leaf gas exchange and water relations among species and tree sizes in an Arizona pine–oak forest. *Tree Physiol.* 20(1):1-12.
50. Anderegg LD & HilleRisLambers J (2016) Drought stress limits the geographic ranges of two tree species via different physiological mechanisms. *Global Change Biol.* 22(3):1029-1045.

51. Callaway RM, DeLucia EH, & Schlesinger WH (1994) Biomass allocation of montane and desert ponderosa pine: an analog for response to climate change. *Ecology* 75(5):1474-1481.
52. Law B, Van Tuyl S, Cescatti A, & Baldocchi D (2001) Estimation of leaf area index in open-canopy ponderosa pine forests at different successional stages and management regimes in Oregon. *Agric. For. Meteorol.* 108(1):1-14.
53. Anderegg WR, *et al.* (2018) Woody plants optimise stomatal behaviour relative to hydraulic risk. *Ecol. Lett.* 21:968-977.
54. Irvine J, Law BE, Anthoni PM, & Meinzer FC (2002) Water limitations to carbon exchange in old-growth and young ponderosa pine stands. *Tree Physiol.* 22:189-196.
55. Panek JA & Goldstein AH (2001) Response of stomatal conductance to drought in ponderosa pine: implications for carbon and ozone uptake. *Tree Physiol.* 21(5):337-344.
56. Williams M, Law BE, Anthoni PM, & Unsworth MH (2001) Use of a simulation model and ecosystem flux data to examine carbon-water interactions in ponderosa pine. *Tree Physiol.* 21:287-298.
57. Schubert GH (1974) *Silviculture of southwestern ponderosa pine: the status of knowlege* (US Department of Agriculture, Forest Service, Rocky Mountain Forest and Range Experiment Station, Fort Collins, CO) p 71.
58. Koepke DF & Kolb TE (2013) Species variation in water relations and xylem vulnerability to cavitation at a forest-woodland ecotone. *For. Sci.* 59(5):524-535.
59. Bouffier LA, Gartner BL, & Domec JC (2003) Wood density and hydraulic properties of ponderosa pine from the Willamette valley vs. the Cascade mountains. *Wood and Fiber Science* 35(2):217-233.
60. Domec JC & Gartner BL (2003) Relationship between growth rates and xylem hydraulic characteristics in young, mature and old-growth ponderosa pine trees. *Plant, Cell Environ.* 26:471-483.
61. Hubbard RM, Ryan MG, Stiller V, & Sperry JS (2001) Stomatal conductance and photosynthesis vary linearly with plant hydraulic conductance in ponderosa pine. *Plant, Cell Environ.* 24:113-121.
62. Maherali H & DeLucia EH (2000) Xylem conductivity and vulnerability to cavitation of ponderosa pine growing in contrasting climates. *Tree Physiol.* 20(13):859-867.
63. Love DM, *et al.* (2019) Dependence of aspen stands on a subsurface water subsidy: implications for climate change impacts. *Water Resour. Res.* 55(3):1833-1848.
64. Voicu MC & Zwiazek JJ (2009) Inhibitor studies of leaf lamina hydraulic conductance in trembling aspen (Populus tremuloides Michx.) leaves. *Tree Physiol.* 30(2):193-204.
65. Way DA, Domec JC, & Jackson RB (2013) Elevated growth temperatures alter hydraulic characteristics in trembling aspen (Populus tremuloides) seedlings: implications for tree drought tolerance. *Plant, Cell Environ.* 36(1):103-115.
66. Darbah JN, *et al.* (2010) Will photosynthetic capacity of aspen trees acclimate after long-term exposure to elevated CO2 and O3? *Environ. Pollut.* 158(4):983-991.

67. Gifford GF (1966) Aspen root studies on three sites in northern Utah. *Am. Midl. Nat.* 75(1):132-141.
68. Hall RJ, Davidson DP, & Peddle DR (2003) Ground and remote estimation of leaf area index in Rocky Mountain forest stands, Kananaskis, Alberta. *Can. J. Remote Sens./J. Can. Teledetect.* 29(3):411-427.
69. Sack L & Holbrook NM (2006) Leaf hydraulics. *Annu. Rev. Plant Biol.* 57:361-381.
70. Benomar L, *et al.* (2015) Fine-scale geographic variation in photosynthetic-related traits of *Picea glauca* seedlings indicates local adaptation to climate. *Tree Physiol.* 35:864-878.
71. Benomar L, *et al.* (2016) Genetic adaptation vs. ecophysiological plasticity of photosynthetic-related traits in young *Picea glauca* trees along a regional climatic gradient. *Front. Plant Sci.* 7:48.
72. Benomar L, *et al.* (2018) Thermal acclimation of photosynthesis and respiration of southern and northern white spruce seed sources tested along a regional climatic gradient indicates limited portential to cope with temperature warming. *Ann. Bot.* 121:443-457.
73. Stinziano JR & Way DA (2017) Autumn photosynthetic decline and growth cessation in seedlings of white spruce are decoupled under warming and photoperiod manipulations. *Plant, Cell Environ.* 40:1296-1316.
74. Laur J & Hacke UG (2014) Exploring *Picea glauca* aquaporins in the context of needle water uptake and xylem refilling. *New Phytol.* 203:388-400.
75. Reblin JS & Logan BA (2015) Impacts of eastern dwarf mistletoe on the stem hydraulics of red spruce and white spruce, two host species with different drought tolerances and responses to infection. *Trees* 29:475-486.
76. Schoonmaker AL, Hacke UG, Landhausser SM, Lieffers VJ, & Tyree MT (2010) Hydraulic acclimation to shading in boreal conifers of varying shade tolerance. *Plant, Cell Environ.* 33:382-393.
77. Chason JW, Baldocchi DD, & Huston MA (1991) A comparison of direct and indirect methods for estimating forest canopy leaf area. *Agric. For. Meteorol.* 57:107-128.
78. Johnson DM, McCulloh KA, Meinzer FC, Woodruff DR, & Eissenstat D (2011) Hydraulic patterns and safety margins, from stem to stomata, in three eastern US tree species. *Tree Physiol.* 31(6):659-668.
79. Kosugi Y, Shibata S, & Kobashi S (2003) Parameterization of the CO_2 and H_2O gas exchange of several temperate deciduous broad-leaved trees at the leaf scale considering seasonal changes. *Plant, Cell Environ.* 26:285-301.
80. Wullschleger SD, Norby RJ, & Gunderson CA (1992) Growth and maintenance respiration in leaves of *Liriodendron tulipifera* L. exposed to long-term carbon dioxide enrichment in the field. *New Phytol.* 121:515-523.
81. Tromp-van Meerveld HJ & McDonnell JJ (2006) On the interrelations between topography, soil depth, soil moisture, transpiration rates and species distribution at the hillslope scale. *Advances in Water Resources* 29(2):293-310.
82. Black TA (2016) FLUXNET2015 CA-Obs Saskatchewan-Western Boreal, Mature Black Spruce. FluxNet; The University of British Columbia. DOI: 10.18140/FLX/1440044.

83. Goldstein A (2016) FLUXNET2015 US-Blo Blodgett Forest. FluxNet; Univ. of California, Berkeley, CA (United States). DOI: 10.18140/FLX/1440068.
84. Massman B (2016) FLUXNET2015 US-GLE GLEES. FluxNet. USDA Forest Service. DOI: 10.18140/FLX/1440069.
85. Munger JW (1991-2012) FLUXNET2015 US-Ha1 Harvard Forest EMS Tower (HFR1). DOI: 10.18140/FLX/1440071.
86. Law B (2016) FLUXNET2015 US-Me2 Metolius mature ponderosa pine. United States. DOI:10.18140/FLX/1440079.
87. Novick K & Phillips R (1999-2014)) FLUXNET2015 US-MMS Morgan Monroe State Forest. DOI: 10.18140/FLX/1440083.
88. Blanken P (1998-2014) FLUXNET2015 US-NR1 Niwot Ridge Forest (LTER NWT1). DOI: 10.18140/FLX/1440087.
89. Desai A (1995-2014) FLUXNET2015 US-PFa Park Falls/WLEF. DOI: 10.18140/FLX/1440089.
90. Desai A (2001-2014) FLUXNET2015 US-Syv Sylvania Wilderness Area. DOI: 10.18140/FLX/1440091.
91. Gough C, Bohrer G, & Curtis P (2000-2014) FLUXNET2015 US-UMB Univ. of Mich. Biological Station. DOI: 10.18140/FLX/1440093.
92. Desai A (1999-2014) FLUXNET2015 US-WCr Willow Creek. DOI: 10.18140/FLX/1440095.